VOLCANOGENIC Zn-Pb±Cu MASSIVE SULFIDE DEPOSITS IN THE UPPER CRETACEOUS PLUTO-NOVOLCANIC ARC IN CENTRAL PERU

Dr. Lluís FONTBOTÉ

University of Geneva
Switzerland

C.V.

Lluís Fontboté is Professor of Economic Geology at the University of Geneva Switzerland (Ginebra en español) where he was also Vice-Dean of the Faculty of Sciences and President of the Section Earth and Environmental Sciences.

He graduated in the University of Granada, Spain, and obtained his doctorate from the University of Heidelberg, Germany. He has edited two books and is author of numerous publications in peer-reviewed journals. His current focus is on the genesis of polymetallic ore deposits related to porhyry systems, Iron Oxide Copper Gold deposits an on Mississippi Valley Deposits. He directs the Geneva Ore deposit Group (http://www.unige.ch/sciences/terre/mineral/ore/min_ore.html). Coworkers and graduate students work on research projects in different parts of the world in cooperation with several mining companies and state institutions on a variety of ore deposit types.

Lluís Fontboté was President for 2012 of the Society of Economic Geologists.

Volcanogenic Zn-Pb±Cu massive sulfide deposits in the Upper Cretaceous plutono-volcanic arc in central Peru

Lluís Fontboté[1]

[1] Department of Earth Sciences, University of Geneva, Switzerland, (lluis.fontbote@unige.ch)

1. Introduction and abstract

Several Zn-Pb±Cu volcanogenic massive sulfide (VMS) deposits occur in Cretaceous rocks in the coastal region of Peru (Fig. 1). They include the mid Cretaceous Tambogrande VMS deposit in the Lancones basin in northern Peru (Winter 2010) and, in the Western Peruvian Trough (Atherton et al., 1883), from north to south, the deposits of Maria Teresa (Zn-Pb-Ag-Cu-Ba, Pichardo et al., 2019), Aurora Augusta (Ba-Zn-Pb-Cu, Vidal, 1987), Perubar (Zn-Pb-Ba, Vidal 1987; Polliand et al., 2005; Polliand 2006), and Palma (Zn-Pb-Ba, Steinmüller et al., 2000; Farfán et al., 2019), all now attributed to the uppermost Cretaceous. Whereas Perubar and Maria Teresa occur in volcano-sedimentary sequences, the host rock at Maria Teresa are volcanic and subvolcanic rocks. In a volcano-sedimentary sequence of attributed mid Cretaceous age, occurs the deposit of Cerro Lindo (Zn-Cu-Pb, Gariépy and Hinostroza, 2003; Votorantim, 2017; Bueno Carreón and Mendoza Mondragón, 2019).

Recent positive exploration results (e.g. Farfán et al., 2019, Pichardo et al., 2019) indicate that the uppermost Cretaceous VMS belt in central Peru is underexplored. In this contribution, aspects concerning the geological setting, alteration, and timing of mineralization at Maria Teresa, Perubar, and Palma VMS deposits are discussed partly on the basis of descriptions contained in Polliand et al. (2005), Polliand (2006), Pichardo et al. (2019), and Farfán et al. (2019) that are not repeated here. Several common patterns arise and can be integrated in a genetic model pointing to ore deposit formation in the Upper Cretaceous plutono-volcanic arc itself (not in a marginal arc as previously proposed) possibly by sub-seafloor mixing of hydrothermal fluids of magmatic origin with coeval seawater.

2. Age, composition, and setting of host rocks at the Maria Teresa, Perubar, and Palma VMS deposits

The high resolution U-Pb in zircon geochronological work by Polliand et al. (2005) yielded ages of 69.71±0.18 Ma y 68.92±0.16 Ma for rhyolitic lavas at the bottom and top of the Perubar ore bodies. These ages broke the paradigm that the volcanic rocks host of the VMS deposits in this part of the belt were of Lower or mid Cretaceous age ("Casma Group"). The data showed further that mafic and felsic volcanic and subvolcanic host rocks were roughly coetaneous with the large Inclinado monzodiorite porphyry intrusion (67.89±0.18 Ma), thought to be responsible of the contact metamorphism affecting part of the ore deposit. Polliand et al. (2005) concluded that "basin subsidence, submarine volcanism and plutonic activity occurred in close spatial and temporal relationship within the Andean magmatic arc during the Late Cretaceous" and that the Perubar deposit was not emplaced in a "marginal basin" (Vidal, 1987) but in a pull-apart basin located in the "plutono-volcanic arc".

Other dating support an uppermost Cretaceous age for this part of the VMS belt. Vidal (1987, sample AA3) published K-Ar ages of 68±2 and 63±2 Ma on quartz-sericite haloes in the Aurora Augusta VMS deposit that were similar to those subsequently determined at Perubar (Polliand et al., 2005). Vidal (1987) interpreted these uppermost Cretaceous ages to result from thermal resetting and, following the prevailing assumption that host rock at Perubar was of mid Cretaceous age and did belong to the Casma Group, proposed mineralization to take place at 106 and 116 m.y. (his sample AA2). At Maria Teresa, Romero et al.

(2008) reported an upper-most Cretaceous age (68 ± 6 Ma, Rb/Sr on hydrothermal sericite). Also, as summarized by Farfán et al. (2019), the age of the Palma VMS deposit is attributed to the uppermost Cretaceous on the basis of lithostratigraphic correlation with the Perubar deposit located 15 km to the north and with Quilmaná basalts in the north flank of the Mala River, where an $^{40}Ar/^{39}Ar$ whole rock "approximate age of 67.6 Ma" (Maestrichtian) has been published by Noble et al. (2005).

To account that the volcanism is uppermost Cretaceous (to Paleocene), Romero et al. (2008) propose using the term "Upper Cretaceous-Paleocene Volcano-Sedimentary sequence" instead of Casma Group (Albian-Cenomanian) for the host rocks of Maria Teresa and Palma.

Along similar lines, Cueva et al. (2010) describe calc-alkaline "andesites and dacites" in "Maestrichtian-Danian sequences" between Pucusani and Chimbote that would occur east of the Coastal Batholith (this appears not to be everywehre the case as the Maria Teresa deposit occurs west of the main part of it). These authors propose to restrict the term "Casma Group" to the Albian_Cenomanian (~108-93 Ma) volcano-sedimentary sequences showing tholeitic and calc-alkaline signatures occurring west of the Coastal Batholith.

Together with pelitic rocks partly rich in organic matter and subordinate limestones, the main host rocks of the Perubar, and Palma VMS deposits are submarine volcanic and subvolcanic rocks, showing in places peperitic textures. Host rock at Maria Teresa are only subvolcanic and volcanic rocks, some of them as pillow and blocky lavas typical of submarine delta fans. Since most volcanic and subvolcanic host rocks at the Maria Teresa, Perubar, and Palma VMS deposits are hydrothermally altered, major element geochemistry is of limited use. Discrimination diagrams based on immobile elements of selected samples show that composition of the volcanic and subvolcanic host rocks in the three deposits are indistinguishable (Fig. 2) showing certain bimodality (basalts to andesites vs. dacites to rhyodacites). Further, all the analyzed samples plot in the field of calc-alkaline volcanic arc basalts (Fig. 3). Tholeitic signatures typical of spreading in marginal basins are not found.

The spatial coincidence of the studied uppermost Cretaceous VMS deposits with the volcano-plutonic arc and the results plotted in Fig. 3 differ from the ones at the mid Cretaceous VMS deposit of Tambogrande (Winter, 2008). There, most host rocks plot also in the field of calc-alkaline volcanic arc basalts but closer to the Zr/117 corner and a fraction of the volcanic host rocks plot in the field of tholeitic volcanic arc basalts. Winter et al. (2010) propose that Tambogrande was emplaced in a trough related tectonically to the break-up of Gondwana in which volcanism and associated VMS deposits formed in a marginal basin as a consequence of a rifting process "due to a westward and oceanward retreating arc, resembling a Mariana arc-type setting".

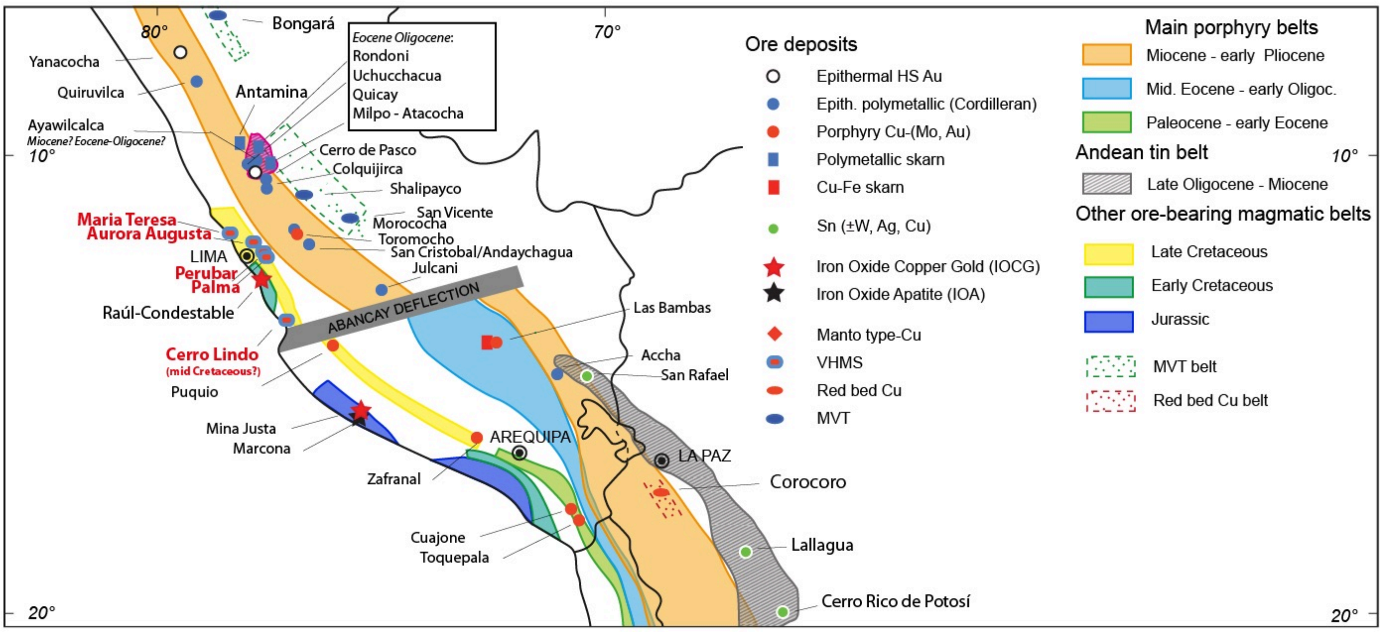

Fig. 1. Sketch showing Upper Cretaceous VMS deposits (in red) in Central Peru and other selected ore deposits (from Fontboté, 2018, modified). Note that porphyry deposits occur in the southern continuation of the Upper Cretaceous magmatic arc.

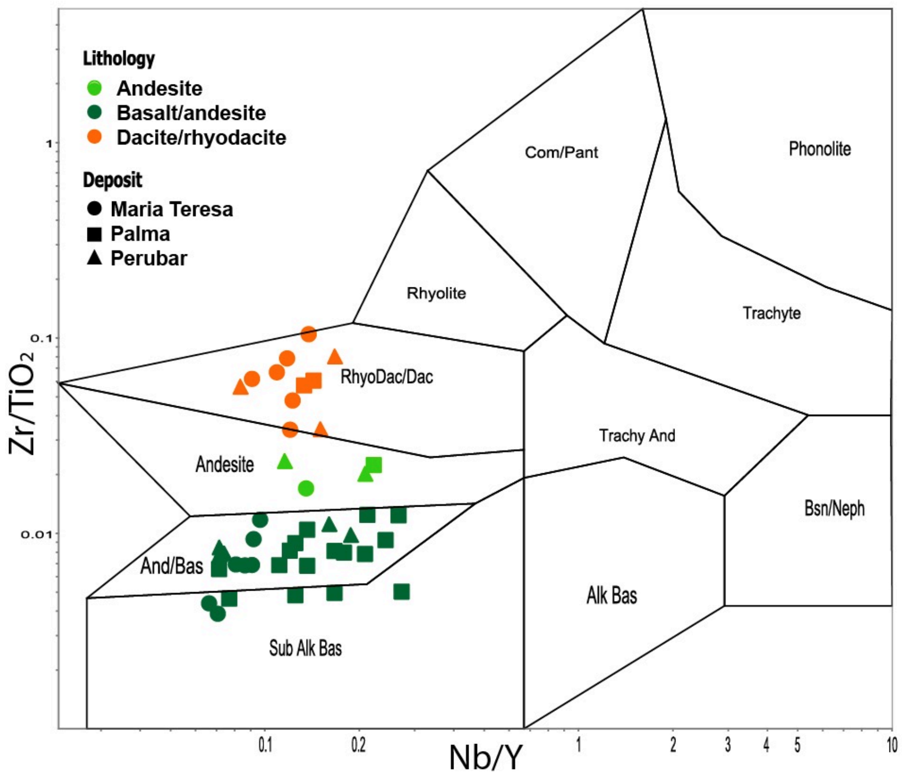

Fig. 2 Volcanic and subvolcanic host rocks at the Maria Teresa, Perubar, and Palma VMS deposits plotted in the Zr/TiO_2 vs. Nb/Y discrimination diagram of Winchester y Floyd (1977). Note the compositional similarity among the deposits. Analyses in Table1.

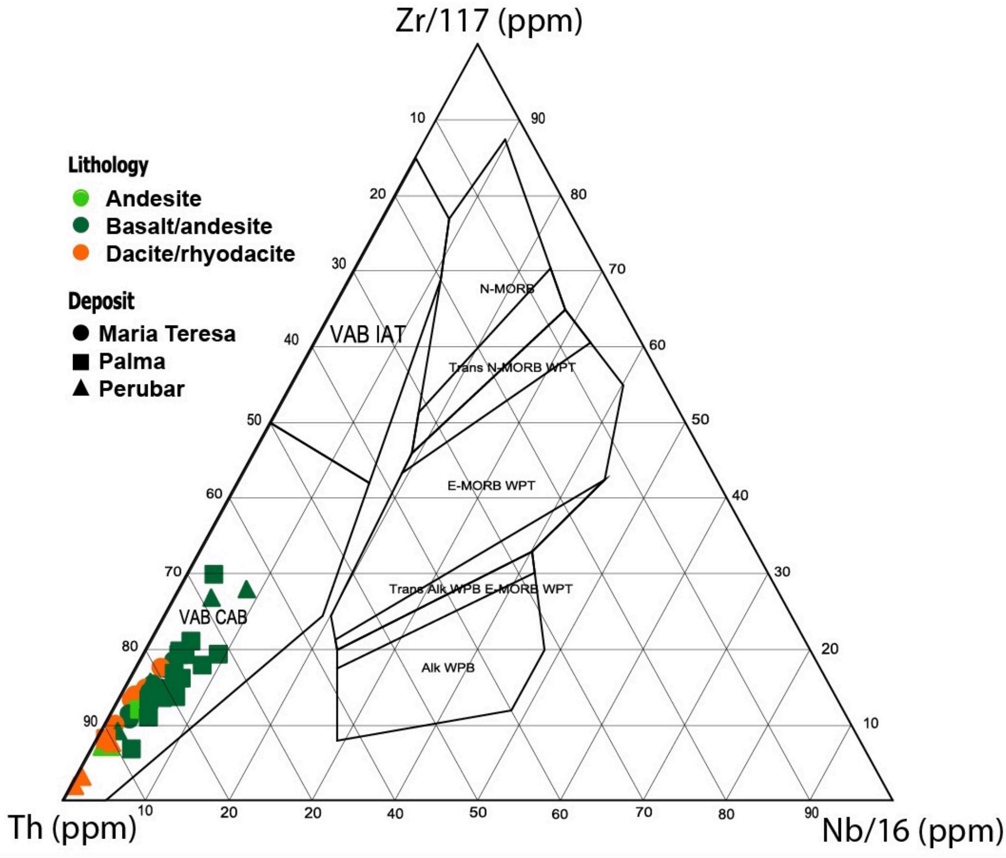

Fig. 3 Discrimination diagram Th-Zr/117-Nb/16 of Wood (1980). All analyzed samples plot in the field of volcanic arc calc-alkaline basalts. Note that the original diagrams of Wood (1979, 1980) used Hf/4 and Ta, values commonly substituted by Zr/117 and Nb/116 given that reliable analyses of Zr and Nb are more frequent. Same data as in Fig. 2. VAB CAB: Volcanic arc calc-alkaline basalts; VAB IAT: Island-arc tholeiitic basalts, WPB: Within plate tholeiite; WPB: Within plate basalts.

Table 1. Whole rock XRF analyses (laboratories Universities of Geneva and Lausanne) of volcanic and subvolcanic rocks of the VMS deposits of Maria Teresa, Perubar and Palma. Most possible least altered samples have been selected. Alteration indexes AI and CCPI according Large et al. (2001) are indicated for control

Deposit	Sample	East	North	masl	Lithology	Alteration	AI	CCPI	SiO2	TiO2	Al2O3	Fe2O3	MnO	MgO	CaO	Na2O	K2O	P2O5	LOI	Zr	Nb	Y	Th	Ba	Sr	Rb	Cu	Zn	Pb	Total
									%	%	%	%	%	%	%	%	%	%	%	ppm	ppm	ppm	ppm	ppm	ppm	ppm	ppm	ppm	ppm	%
Maria Teresa[1]	10909-E	251205	8730034	221	Basalt/andesite	Least altered	26.1	72.3	54.21	1.13	17.82	10.29	0.19	3.32	5.04	4.99	0.23	0.20	2.10	78	2.1	26	3	1122	324	4	91	141	12	99.68
Maria Teresa[1]	10910-E	251234	8729118	282	Basalt/andesite	Least altered	26.7	69.7	57.40	1.02	16.45	9.30	0.18	3.33	3.97	5.41	0.09	0.22	2.23	70	2.2	26	3	137	200	2	103	123	7	99.65
Maria Teresa[1]	10911-E	251563	8728525	284	Basalt/andesite	Least altered	22.6	68.9	59.94	1.17	14.37	10.37	0.23	2.49	3.00	5.74	0.06	0.30	2.23	110	3.2	35	4	38	98	<DL	54	145	7	99.97
Maria Teresa[1]	10914-E	252571	8728495	248	Andesite	Least altered	39.9	77.5	55.26	0.74	15.16	9.39	0.17	5.69	7.73	2.97	1.40	0.13	1.31	126	3.3	24	7	828	284	25	56	90	16	100.09
Maria Teresa[1]	10916-E	251367	8728853	99	Basalt/andesite	ab±ep±chl	37.6	90.9	48.92	1.12	15.39	13.00	0.32	6.11	9.70	1.36	0.54	0.11	2.79	49	1.3	20	2	1379	229	11	178	120	14	99.56
Maria Teresa[1]	10918-E	251566	8727991	86	Basalt/andesite	ab±ep±chl	40.1	86.3	47.59	0.87	17.73	12.33	0.21	5.33	8.80	1.34	1.46	0.10	3.86	60	1.5	17	4	360	194	31	85	108	8	99.70
Maria Teresa[1]	10920-E	252937	8728589	134	Basalt/andesite	Least altered	33	82.9	54.23	0.57	14.31	8.59	0.19	7.01	11.44	3.08	0.14	0.05	0.45	22	0.7	10	2	271	200	3	90	81	7	100.12
Maria Teresa[1]	10921-E	251120	8728033	-190	Dacite/rhyodacite	Least altered	40.6	61.4	63.62	0.46	13.65	5.35	0.30	1.54	4.80	1.54	2.80	0.09	5.20	222	4.9	40	11	1478	40	59	33	136	9	99.54
Maria Teresa[1]	10922-E	251576	8728558		Dacite/rhyodac*	Least altered	37.8	23.6	74.59	0.19	12.70	1.91	0.03	0.35	1.00	4.37	2.92	0.03	1.10	148	2.2	19	11	2376	77	38	4	21	11	99.45
Maria Teresa[1]	10923-E	251492	8728248	-175	Basalt/andesite	Least altered	34.8	69.7	57.30	0.95	15.91	9.40	0.27	3.09	3.53	4.32	1.10	0.28	3.40	111	3.3	34	5	531	137	23	74	153	12	99.66
Perubar[2)]	MPP625	328157	868333	1035	Basalt/andesite	Least altered	36.3	74.3	49.40	0.93	18.01	11.95	0.18	3.71	7.84	2.97	2.44	0.15	1.99	74	0.7	27	6	1715	321	79	184	764	157	99.90
Perubar[2)]	MPP377	328958	8683064	1340	Basalt/andesite	Least altered	38.9	64.8	52.03	1.07	17.35	6.91	0.25	4.13	8.02	3.07	2.93	0.17	1.18	91	0.7	28	4	9663	367	97	14	292	110	98.18
Perubar[2)]	MPP350	329431	8683514	1450	Basalt/andesite	Least altered	34.3	75	52.77	0.92	16.28	9.35	0.15	4.94	8.20	3.57	1.20	0.27	1.32	103	2	25	2	737	539	37	37	101	30	99.13
Perubar[2)]	MPP707	329252	8683417	997	Basalt/andesite	Least altered	22.3	74.1	51.87	1.17	17.20	9.52	0.14	3.44	10.14	3.92	0.61	0.17	0.42	92	0.7	28	2	425	402	28	11	160	36	98.71
Perubar[2)]	MPP315	328999	8683372	1200	Basalt/andesite	chl-py-(ser)	72.3	91.4	46.8	0.77	15.5	18.66	0.3	9.1	1.15	2.41	0.19	0.22	3.3	76	9	16	3	1430	109	15	12	1013	454	98.73
Perubar[2)]	MPP611	329178	8683353	1196	Andesite	chl-py-(ser)	46.7	73.9	57.5	0.75	15.4	10.69	0.16	6.04	2.17	5.36	0.56	0.2	0.7	177	8	26	19	336	181	31	84	394	107	99.63
Perubar[2)]	MPP323	329171	8682515	1277	Andesite	Least altered	35.5	59.1	59.5	0.65	15.6	6.71	0.14	2.41	5.61	3.63	2.68	0.19	1.3	132	5	24	14	4954	380	95	64	390	131	98.99
Perubar[2)]	MPP521	329254	8682569	1002	Dacite/rhyodacite	qtz-ser-K feld	81.3	10	56.1	0.21	17.8	0.99	0.05	0.33	2.35	0.37	11.5	0.08	2.1	119	0.7	24	47	66700	240	316	86	47	23	98.56
Perubar[2)]	MPP555[2]	329261	8682728	1150	Dacite/rhyodacite	Least altered	24.8	28.1	63.5	0.53	16.3	2.33	0.05	1.21	3.04	6.96	2.08	0.22	1.4	182	9	40	18	4214	235	71	8	42	8	98.05
Perubar[2)]	MPP594[2]	329277	8682617	1107	Dacite/rhyodacite	qtz-ser-K feld	70.7	12.3	74.3	0.11	11.9	0.96	0.01	0.17	1.22	1.54	6.5	0.03	1.2	89	10	12	22	7432	181	219	11	124	63	98.72
		DDH	From (m)	to (m)																										
Palma[3]	PLM0210	DDHPLM1101	141	142	Basalt/andesite	Least altered	24.4	77.8	46.5	1.6	17.1	11.78	0.15	3.89	10.5	3.76	0.7	0.32	3.1	105	1.5	21	2	388			104	38		99.38
Palma[3]	PLM0233	DDHPLM1102	148.9	149.9	Basalt/andesite	Least altered	32.6	66.7	55.2	1.26	15.6	8.86	0.29	3.15	4.74	4.62	1.37	0.2	2.8	86	3	22	4	3699			62	436		98.51
Palma[3]	PLM0243	DDHPLM1202	112	114	Basalt/andesite	Least altered	17.8	76.3	53.1	1.23	13.2	9.62	0.4	2.98	11	3.71	0.2	0.36	2.8	57	2	26	2	142			64	604		98.80
Palma[3]	PLM0267	DDHPLM1202	54.88	56.88	Basalt/andesite	Least altered	19.4	64.6	53.5	1.19	15.4	7.52	0.17	3.06	9.53	5.3	0.51	0.47	2.2	97	3	25	3	438			175	62		98.93
Palma[3]	PLM0296	DDHPLM1203	117.5	119	Basalt/andesite	Least altered	27.8	69.3	52.4	1.2	16.1	9.38	0.22	3.49	7.35	4.59	1.1	0.28	2.3	107	3	24	4	504			57	124		98.50
Palma[3]	PLM0244	DDHPLM1202	24.9	26.9	Dacite/rhyodac*	Least altered	19.8	34.7	74.5	0.21	12.3	2.47	0.04	0.88	0.87	5.59	0.71	0.03	1.1	120	2	15	11	276			49	27		98.81
Palma[3]	PLM0276	DDHPLM1203	299.13	301.13	Dacite/rhyodac*	Least altered	15.4	27.7	75.3	0.2	12.2	1.95	0.07	0.6	1.37	5.91	0.73	0.01	1	121	2	14	11	568			63	14		99.36
Palma[3]	PLM0276	DDHPLM1203	315.1	317.1	Dacite/rhyodac*	Least altered	19.9	53.3	64	0.51	16.1	5.34	0.14	1.6	4.14	5.32	0.75	0.19	1.2	114	4	18	7	551			18	41		99.38
Palma[3]	PLM0230	DDHPLM1101	153.95	155	Basalt/andesite	Least altered	27.1	75.7	50	1.14	17.1	10.7	0.47	4.27	8.58	4.3	0.51	0.15	2	55	2	16	3	542			33	325		99.26
Palma[3]	PLM0343	DDHPLM1204	551.5	552.6	Basalt/andesite	Least altered	28.1	79.2	52.3	1.47	14.4	12.94	0.24	3.74	7.83	3.64	0.75	0.22	0.7	101	3	27	3	588			275	81		98.38
Palma[3]	FPE365	PA-EX-08/186	59.05	59.15	Basalt/andesite	Least altered	31.7	69.2	52.36	0.73	18.72	7.61	0.17	3.91	7.73	3.74	1.40	0.12	2.93	76	3	22	3	1739	389	37	115	98	4	99.66
Palma[3]	FPE366	PA-EX-09/185	35.79	35.85	Basalt/andesite	Least altered	33.2	67.5	54.06	1.03	18.24	7.43	0.10	3.97	6.67	4.10	1.38	0.18	2.08	127	8	30	4	1020	416	42	46	108	17	99.42
Palma[3]	FPE372	PA-EX-15/185	82.5	82.57	Basalt/andesite	Least altered	23.5	76.8	50.92	1.51	14.27	12.36	0.21	3.63	11.07	3.87	0.95	0.27	0.27	139	8	33	9	1320	287	17	50	116	15	99.52
Palma[3]	FPE375	PA-EX-15/185	207.78	207.84	Basalt/andesite	Least altered	27.4	73.1	52.26	1.07	17.49	9.29	0.22	4.28	8.12	4.51	0.48	0.16	1.72	87	4	24	4	605	473	14	8	107	15	99.73
Palma[3]	FPE378	PA-EX22/1857	263.09	263.14	Basalt/andesite	Least altered	24.7	73.5	52.09	1.27	16.42	11.33	0.25	3.89	7.30	5.26	0.24	0.18	1.40	64	6	22	7	150	195	7	111	109	4	99.69

1) Additional data in PIcardo et al., 2019). 2) Data from Polliand (2006) complemented for some elements with archive data of University of Geneva. 3) Analyses of additional samples are published by Farfán et al. (2019).

*) Dyke

Further work, in particular on not altered rocks, should reveal if the clear calc-alkaline signature of the three studied uppermost Cretaceous VMS deposits in central Peru, typical for a subduction-related mature magmatic arc, and also found in the Cretaceous Coastal Batholith (Pitcher et al., 1985), represent a change from marginal basin conditions that could have prevailed in mid Cretaceous times (Atherton et al. 1983; Cueva et al., 2010). The recent recognition of Grenville basement in the forearc of central Peru (Romero et al., 2013) should be also considered.

3. Hydrothermal alteration and contact metamorphism

At Maria Teresa, where the host is devoid of sedimentary rocks, the alteration pattern affecting volcanic and subvolcanic rocks is particularly clear. The ore bodies, planar to irregular with "root" zones, occur in a sub-horizontal "prospective horizon" outlined by an alteration front between intense sericitization (±chlorite) at the footwall of the ore bodies (Fig. 4) and epidote-albite-chlorite-carbonates in the hanging wall and distal parts This assemblage typical of ocean floor hydrothermal alteration of mafic and andesitic rocks (e.g., Alt et al., 2010) is also observed in areas remote of mineralization. The sericite alteration below the richest ore bodies is particularly intense, with Ishikawa et al. (1976) alteration index values over 90. The "prospective horizon" is interpreted as a paleo-horizon in which hydrothermal fluids ascending along N150E feeders mixed with seawater percolating in the volcanic pile. At Perubar and Palma sericitic alteration is also present, but less developed and only observed at the footwall of certain areas close to feeders.

Fig. 4 Intense sericitic alteration affecting basalts and basaltic andesites at the footwall of Sofia D ore body in the Maria Teresa mine. Note strong foliation. Width of picture: 5 m (back part).

In the three studied deposits the ore and host rock are affected by contact metamorphism with development of pyrrhotite and magnetite, and when limestone present in the host sequence (Perubar and Palma) of calc-silicates (Vidal, 1987; Polliand et al., 1999; Farfán et al., 2019). At Maria Teresa, contact metamorphism over previously sericitized volcanic rocks yields a typical mottled texture containing biotite, garnet, and cordierite (Fig. 5) The consistent occurrence of contact metamorphism produced by the batholith intrusions is another argument for suggesting that the ore deposits are located at the magmatic arc.

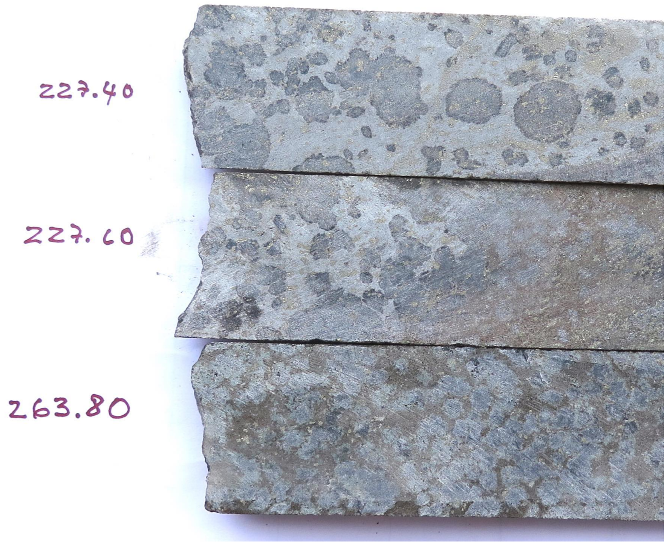

Fig. 5 Mottled texture with biotite, cordierite, garnet, pyrite and pyrrhotite (Schmidt, 2017) developed occurring beneath alteration front. This assemblage is typical for sericitic alteration on andesitic rocks affected by contact metamorphism (Shanks, 2012). Maria Teresa, DDH17S, hole meters as indicated in picture. Each drill core is 8 cm wide.

4. Dikes and feeders of ore-bearing fluids

A striking feature recognized by recent surface mapping both at the Palma and Maria Teresa VMS deposits (Farfán et al., 2019, Pichardo et al., 2019), is the occurrence at regional scale of sets of roughly parallel dikes of mafic and felsic composition that are perpendicular to bedding and that trend NS to N160E (Palma) and N150E (Maria Teresa). At Palma, although mapped in less detail, these dikes also show a similar pattern. In the three deposits, mafic dikes are crosscut by pyrite±pyrrhotite and Zn-Pb±Cu mineralization and at Colquisiri dacitic dikes are also affected by the sericitic alteration accompanying mineralization (e.g. samples 10401E and 2806 in Table 1 of Pichardo et al., 2019). This suggests that the hydrothermal system responsible for ore formation was at least partly active during dike emplacement. The U-Pb age of 67.91±0.17 delivered by zircons of a dacitic dike at Palma, very close to the obtained ages on volcanic flows, is consistent with this hypothesis (Polliand et al., 2005).

These uppermost Cretaceous dike swarms outline a geometry similar to that recognized in several places in the western margin of the South American plate, as for example calc-alkaline Jurassic dikes in northern Chile (Lucassen and Franz, 1994). The dike geometry could reflect an extensional setting (Calderón et al., 2007), but there is also increasing evidence that during oblique plate subduction, dikes and in general volcanic arcs can be emplaced along strike-slip structures parallel to the transpressional margin (e.g., Tibaldi et al., 2010; Spacapan et al., 2016).

At Maria Teresa, where no sedimentary rocks disturb observation, the ore bodies show a clear N150E elongation, parallel to the main dike orientation (Fig. 1 in Pichardo et al. 2019). The intense sericitic alteration typical of this deposit follows also this orientation. These observations, together with ore grade mapping of the Sofia D body (Minera Colquisiri, unpublished reports) revealing highest copper grade centers at the contact and along andesitic dikes, strongly suggest that the feeders of the ore-forming fluids used the same conduits than the dikes. At Palma, as mentioned above, mafic and felsic dikes display a similar pattern. Particular elongations of the ore bodies have not been recognized so far, possibly partly because of lack of data and partly because the sedimentary host rock favors bed-parallel replacement. At Perubar, already Polliand et al. (2005) proposed ore emplacement in a pull-apart basin triggered by strike-slip dextral faulting. The elongated morphology of the ore bodies recognized in the maps of Cerro Lindo (Votorantim, 2017; Fig. 1 of Bueno Carreón and Mendoza Mondragón, 2019) resembles strongly the one at Colquisiri.

5. Relative timing of mineralization

In Maria Teresa and Palma there are evidences suggesting subseafloor replacement under significant overburden (Pichardo et al., 2019; Farfán et al., 2019). At both deposits, veins containing sphalerite and galena crosscut andesitic dikes (Figs. 6 and 7) that continue upwards tens to hundreds meters above the main mineralized horizons. At Colquisiri, as indicated above, dacitic veins are affected by the intense sericitic alteration. At Palma, alteration and mineralization also affects andesitic sills and dikes, but their vertical continuity over the mineralized horizon has not been followed so far in detail. However, the age of the measured rhyodacitic dike mentioned above, 1 Ma apart or less of the host lava flows, is also consistent with the hypothesis that dacitic dikes were emplaced when the hydrothermal system was still active.

6. Concluding remarks.

The studied uppermost Cretaceous VMS deposits in the Coastal region of central Peru were emplaced at the volcanic-plutonic arc or very close of it as indicated by the spatial and temporal coincidence of volcanic and subvolcanic rocks and intrusive bodies belonging to the Coastal Batholith. The consistent calc-alkaline signature found in the mafic and felsic volcanic and subvolcanic host rocks in Maria Teresa, Perubar, and Palma is consistent with this hypothesis.

Fig. 6 Chalcopyrite, sphalerite, and galena cross-cutting and replacing an andesitic dike. Maria Teresa deposit, Sofia D ore body, SN38 145S.

Fig. 7 Pyrrhotite, sphalerite, and galena vein cross-cutting an andesitic dike in the Santa Lidia sector of the Palma deposit (DDHSL-15001, 479 m). Width of picture: 14 cm.

The swarms of parallel dikes, roughly coetaneous with mineralization, occurring at Maria Teresa and Palma may reflect emplacement in an overall transpresional environment triggered by oblique subduction. Intersection with crosscutting NE and NW trending structures probably control the location of the main mineralization centers and of pull-apart basins in which the VMS deposits have been emplaced. At the Maria Teresa VMS deposit, in a site devoid of sedimentary rocks, the ore replaced volcanic and subvolcanic rocks, whereas the Perubar and Palma VMS deposits were emplaced in volcano-sedimentary sequences deposited in intra-arc basins. Irrespective of the different host rock, the similar characterisitics including the dike geometry and alteration pattern suggests that the ore forming systems were remarkably similar in the three deposits. At Maria Teresa, the lack of sediments favors the intense sericitic alteration. and the elongated morphology of the ore bodies allows to recognize that the ore fluid feeders followed conduits also used by the dike swarms. At Perubar and Palma, similar ore body and dike geometry as well as alteration patterns exist, but their recognition is more difficult, because of the neutralization and dilution effect of still not completely consolidated host sediments.

Sulfur and strontium isotope data (Plliand et al., 1999, Polliand 2006, and unpublished) support mixing between a H_2S-dominated hydrothermal solution with $\partial^{34}S$ close to 0 an $^{87}Sr/^{86}Sr \leq 0.70669$ and coeval seawater as the main mechanism responsible for the precipitation of the sulfide-barite ores. At Palma, negative ∂S ratios (with $\partial^{34}S$ down to 27.3‰) pyrite and pyrrhotite intergrown with framboidal pyrite suggest subordinate incorporation of bacteriogenic reduced sulfur. The replacing evidences and the overall bed-parallel morphology of the main ore bodies suggests that fluid mixing took place predominantly sub-seafloor in planar aquifers controlled by lithology.

The reviewed deposits in central Peru show similarities concerning geological setting, mineral assemblages, zoning, and alteration to active submarine arc-related hydrothermal systems in the Kermadec and Aeolian arcs and at the SuSu Knolls site in the Manus basin where mineralization by magmatic-hydrothermal fluids has been proposed on the basis of extensive evidence (de Ronde et al., 2011, 2014; Petersen et al., 2014; Yeats et al., 2014). At the Maria Teresa, Perubar, and Palma deposits, mineralization by hydrothermal fluids of magmatic origin appears also as the most likely hypothesis. This is supported by their occurrence in the plutono-magmatic arc itself and the involvement of acidic-oxidizing fluids as indicated by the intense sericitic alteration, the tetrahedrite-tennantite rich mineral assemblages, and the presence of enargite at Maria-Teresa (Díaz, 2015). The available sulfur and strontium isotope data are compatible with this view. A magmatic fluid origin was already proposed in the Andes for the intermediate to high sulfidation assemblages of the Au-rich La Plata VMS deposit in Ecuador (Chiaradia et al., 2008). The occurrence in the late Cretaceous magmatic arc located directly south of the VMS belt (Fig. 1) of porphyry copper deposits (Carlotto et al., 2009) is additional evidence compatible with a magmatic affiliation for the VMS deposits considered in the present contribution.

Many of the features discussed above, including the elongated morphology of the ore bodies and the sericitc alteration, are shared by the Cerro Lindo VMS deposit and, possibly, similar conclusions can be drawn.

Acknowledgements

This contribution has greatly benefited from observations by and discussions with the geology and exploration staffs of Volcan Compañía Minera and Minera Colquisiri. Review by S. Rosas (PUCP) is greatly acknowledged.

References

Alt, J.C., Laverne, C., Coggon, R.M., Teagle, D.A.H., Banerjee, N.R., Morgan, S., Smith-Duque, C., Harris, M. y Galli, G. (2010) Subsurface structure of a submarine hydrothermal system in ocean crust formed at the East Pacific Rise, ODP/IODP Site 1256, Geochem. Geophys. Geosyst.11 Q10010.

Atherton, M. P., Pitcher, W. S., and Warden, V. (1983) The Mesozoic marginal basin of central Peru: Nature, v. 305, p. 303-306.

Bueno Carreón, J.P. and Mendoza Mondragón, M. (2019) Caracterización litogeoquímica en el yacimiento VMS - Cerro Lindo y su relación con la mineralización para determinar vectores guías en exploración. Proexplo 2019, Lima, resúmenes extendidos.

Calderon, M., Fildani, A., Herve, F., Fanning, C. M., Weislogel, A., and Cordani, U. (2007) Late Jurassic bimodal magmatism in the northern sea-floor remnant of the Rocas Verdes basin, southern Patagonian Andes. Journal of the Geological Society, v. 164, p. 1011–1022.

Carlotto, V., Quispe, J, Acosta, H., Rodríguez, R., Romero, D., Cerpa, L., Mamani, M., Díaz-Martínez, E., Navarro, P., Jaimes, F., Velarde, T., Lu, S. & Cueva, E. (2009) Dominios Geotectónicos y Metalogénesis del Perú. Bol. Soc. Geol, v. 103, P. 1-89.

Chiaradia, M., Tripodi, D., Fontboté, L., and Reza, B., (2008) Geologic setting, mineralogy, and geochemistry of the Early Tertiary Au-rich volcanic-hosted massive sulfide deposit of La Plata, Western Cordillera, Ecuador: Economic Geology, v. 103, p. 161-183.

Cueva, E., Mamani, M., and Rodríguez, R., (2019) Magmatismo y geoquímica del volcanismo Albiano Cenomaniano (Grupo Casma) y Maastrichtiano-Daniano entre Pucusana y Chimbote. XV Congreso Peruano De Geología, resúmenes extendidos. Sociedad Geológica de Perú, Publ. Esp., v. 9, p. 921-924.

de Ronde, C.E.J., Hein, J.R., and Butterfield, D.A (2014) Metallogenesis and mineralization of intraoceanic arcs II: The Aeolian, Izu-Bonin, Mariana, and Kermadec Arcs, and the Manus Backarc Basin - Introduction. Economic Geology, v. 109, p. 2073-2077.

de Ronde, C.E.J., Massoth, G.J., Butterfield, D.A., Christenson, B.W., Ishibashi,J., Ditchburn, R.G., Hannington, M.D., Brathwaite, R.L., Lupton, J.E., Kamenetsky, V.S., Graham, I.J., Zellmer, G.F., Dziak, R.P., Embley,R.W., Dekov, V.M., Munnik, F., Lahr, J., Evans, L.J., and Takai, K. (2011) Submarine hydrothermal activity and gold-rich mineralization at Brothers volcano, Kermadec arc, New Zealand: Mineralium Deposita, v. 46, p. 541−584.

Díaz, M. (2015) Estudio microscópico de 41 muestras de roca. Informe privado APT para Minera Colquisiri, 100 p.
Farfán, C., Monge, R., and Fontboté, L. (2019) Palma, yacimiento de Zn-Pb tipo VMS en una cuenca intra-arco del Cretácico Superior en Perú central, nuevos avances en exploración para un gran potencial. Proexplo 2019, Lima, resúmenes extendidos.
Fontboté, L. (2018) Ore deposits of the central Andes: Elements, v. 14, no. 4, p. 257-261.
Gariepy, L. and Hinostroza, J. (2013) El yacimiento tipo sulfuro masivo volcanogénico Cerro Lindo, Departamento de Ica, Perú. Proexplo, resumenes extendidos, 23 p.
Ishikawa, Y., Sawaguchi, T., Ywaya, S., and Horiuchi, M. (1976) Delineation of prospecting targets for Kuroko deposits based on modes of volcanism underlying dacite and alteration haloes. Mining Geology, v. 26, p. 105-117.
Large, R.R., Gemmell, J. B., Paulick, H., and Huston, D. L. (2001) The alteration box plot: A simple approach to understanding the relationship between alteration mineralogy and lithogeochemistry associated with volcanic-hosted massive sulfide deposits deposits. Economic Geology, 96, 957–971.
Lucassen, F. and Franz, G. (1994). Arc related Jurassic igneous and meta-igneous rocks in the Coastal Cordillera of northern Chile/Region Antofagasta. Lithos, v. 32, 273–298.
Noble, D., Ríos, A., Vidal, C., Spell, T., Zanetti, K., Ángeles, C., Ochoa, J., and Cruz, S. (2005) Late Cretaceous basalt in the rio Mala valley, central Peru: Evidence for extension and mafic amgmatism prior to Latest Cretaceous-Paleocene plutonism and silicic volcanism. Sociedad Geológica del Perú, volumen Jubilar Alberto Giesecke Matto, 141-148.
Petersen, S., Monecke, T., Westhues, A., Hannington, M.D., Gemmell, J.B., Sharpe, R., Peters, M., Strauss, H., Lackschewitz, K., Augustin, N., Gibson, H., and Kleeberg, R. (2014) Drilling shallow-water massive sulfides at the Palinuro volcanic complex, Aeolian island arc, Italy: Economic Geology, v. 109, p. 2129–2157.
Pichardo, E., Fontboté, L., Mena, T. Chirinos, O., and Halter, W. (2019) El yacimiento de Zn-Pb-Cu-Ag tipo VMS María Teresa, Perú: geología y exploración. Proexplo 2019, extended abstracts, 7 p.
Pitcher, W.S., Atherton, M.P., Cobbing, E.J., Beckinsale, R.D. (1985) Magmatism at a Plate Edge: the Peruvian Andes. Blackie, Glasgow and London, 289 pp.
Polliand, M. (2006) Genesis, evolution, and tectonic setting of the Upper Cretaceous Perubar Ba-Pb–Zn volcanic-hosted massive sulfide deposit, central Peru. Ph.D. Thesis University of Geneva, Terre and Environement, v. 60, 141 p.
Polliand, M., Fontboté, L., and Spangenberg, J. (1999) Tracing back sulfur isotope reequilibration due to contact metamorphism: A case study from the Perubar VMS deposit, Central Peru. In: C.J. Stanley et al. (eds.), Mineral deposits: processes to processing, 5th biennial SGA meeting, London, England, 22-25 August 1999, Balkema, Rotterdam, p. 967-970.
Polliand, M., Schaltegger, U., Frank, M., and Fontboté, L. (2005) Formation of intra-arc volcanosedimentary basins in the western flank of the central Peruvian Andes during Late Cretaceous oblique subduction: field evidence and constraints from U-Pb ages and Hf isotopes. International Journal of Earth Sciences, v. 94, 231-242.
Romero, D., Quispe, J., Carlotto, V. and Tassinari, C. (2008) Los depósitos de la cuenca Maastrichtiano - Daniano: relación con los yacimientos tipo sulfuros masivos volcanogénicos de Pb - Zn - Cu; Perú central. En: Congreso Peruano de Geología, 14, Lima, 2008. CD - ROM. Lima: Sociedad Geológica del Perú, 6 p.
Romero, D., Valencia, K., Alarcón, P., Peña, D., and Ramos, V. A. (2013) The offshore basement of Peru: Evidence for different igneous and metamorphic domains in the forearc. Journal of South American Earth Sciences, 42(C), 47–60. http://doi.org/10.1016/j.jsames.2012.11.003.
Schmidt, S.Th. (2017) Petrography of 10 thin sections and XR diffractrometry of three samples of Maria Teresa Mine, Minera Colquisiri, S.A. Private report, 18 p.
Shanks, W. (2012) Hydrothermal alteration in volcanogenic massive sulfide occurrence model. US Geological Survey Scientific Investigations Report 2010-5070-C. 165-180
Spacapan, J. B., Galland, O., Leanza, H. A., and Planke, S. (2016) Control of strike-slip fault on dyke emplacement and morphology. Journal of the Geological Society, 173, p. 573–576.
Steinmüller, K., Chacón Abad, N., and Grant, B. (2000) Volcanogenic massive sulfides in Peru. In: Sherlock R.L. and Logan M.A.V. VMS Deposits of Latin America: Geological Association of Canada, Mineral Deposits Division. 2 , p. 423–437.
Tibaldi, A., Pasquare , F., and Tormey, D. (2010) Volcanism in reverse and strike-slip fault settings. In: New Frontiers in Integrated Solid Earth Sciences. Springer, Berlin, 315–348.
Vidal, CCE (1987) Kuroko-type deposits in the Middle-Cretaceous marginal basin of central Peru. Econ Geol v. 82, p. 1409–1430.
Votorantim (2017) Cerro Lindo polymetallic mine, NI 43-101 Technical Report on Operations, 315 p.
Winter, L.S. (2008) The genesis of “giant” copper-zinc-gold-silver volcanogenic massive sulphide deposits at Tambogrande, Peru: Age, tectonic setting, paleomorphology, lithogeochemistry and radiogenic isotopes: Unpublished. Ph.D. thesis, Vancouver, Canada, University of British Columbia, 260 p.
Winter, L.S., Tosdal, R.M., Mortensen, J.K., Franklin, and J.M. (2010) Volcanic stratigraphy and geochronology of the Cretaceous Lancones Basin, northwestern Peru: position and timing of giant VMS deposits. Economic Geology, v. 105, 713–742
Winchester, J.A. and Floyd, P. A. (1977) Geochemical discrimination of different magma series and their differentiation products using immobile elements, Chemical Geology, 1977, v. 20, p. 325-343.
Wood D.A. (1980) The application of a Th–Hf–Ta diagram to problems of tectonomagmatic classification and to establishing the nature of crustal contamination of basaltic lavas of the British Tertiary volcanic province: Earth and Planetary Science Letters, v. 50, p. 11-30.
Wood, D.A., Joron, J-L., and Treuil M. (1979) A re-appraisal of the use of trace elements to classify and discriminate between magma series erupted in different tectonic settings, Earth Planet. Sci. Lett. 45 11979) 326 336.
Yeats, C.J., Parr, J.M., Binns, R.A., Gemmell, J.B., and Scott, S.D. (2014) The SuSu Knolls hydrothermal field, eastern Manus basin, Papua New Guinea: An actively forming submarine high sulfidation copper-gold system: Economic Geology, v.109, p. 2207–2226.

VOLCANOGENIC Zn-Pb±Cu MASSIVE SULFIDE DEPOSITS IN THE UPPER CRETACEOUS PLUTONO-VOLCANIC ARC IN CENTRAL PERU

Dr. Lluís FONTBOTÉ

University of Geneva
Switzerland

NOTAS